Eur. Phys. J. A **18**, 159–161 (2003)
DOI 10.1140/epja/i2002-10292-4

THE EUROPEAN PHYSICAL JOURNAL A

Parity-violating electron scattering at MAMI

Strangeness in the nucleon

S. Baunack[a] and the A4 Collaboration

Institut für Kernphysik, Universität Mainz, Becherweg 45, D-55099 Mainz

Received: 30 September 2002 /
Published online: 22 October 2003 –

Abstract. A measurement of the parity-violating asymmetry in elastic scattering of polarized electrons on protons is currently running within the A4 Collaboration at the MAMI facility in Mainz. The aim is to reveal the contribution of strange quarks to the form factors of the nucleon at a $Q^2 = 0.23\,\mathrm{GeV}^2$. The expected asymmetry without strangeness is around 5.4×10^{-6}. After 600 hours of asymmetry data taking, an accuracy of 1×10^{-6} has been achieved.

PACS. 13.40.Gp Electromagnetic form factors – 11.30.Er Charge conjugation, parity, time reversal, and other discrete symmetries – 14.20.Dh Protons and neutrons – 13.60.-r Photon and charged-lepton interactions with hadrons

1 Introduction

Although there is no net strangeness in the nucleon, there is experimental evidence for the contribution of strange quark and antiquark pairs to the properties of the nucleon. From π-N scattering we know that strange quarks contribute to the mass of the nucleon [1], from deep inelastic scattering that there are contributions to spin and momentum of the nucleon. In this experiment, scattering of longitudinal polarized electrons on unpolarized protons is used for the determination of the contribution of the strange quarks to the vector form factors of the nucleon.

Weak interaction leads to a parity-violating (pv) asymmetry in the cross-section of elastic scattering of polarized electrons on unpolarized protons. At energies much smaller than m_Z the leading pv-term comes from the interference of photon and Z_0 exchange and is of the order Q^2/m_Z^2. The different coupling in weak and electromagnetic interaction allows a separation of the strange contribution to the vector form factors of the nucleon, provided the electric (G_E) and magnetic (G_M) form factors of the proton and neutron —or, alternatively, the Sachs form factors F_1 and F_2— are known [2].

The strange contribution can be written as an additive correction to the parity-violating asymmetry without strangeness, A_0:

$$A = A_0 \cdot (1 + a \cdot F_1^\mathrm{s} + b \cdot F_2^\mathrm{s} + c \cdot G_\mathrm{A}^\mathrm{s})\,, \qquad (1)$$

where a, b and c are kinematical factors.

Given the Mainzer Microtron Facility (MAMI) maximum electron energy —at present 855 MeV— Figure of Merit (FOM) calculations led to the scattering angle of $\theta = (35 \pm 5)^\circ$, which corresponds to $Q^2 = 0.227\ \mathrm{GeV}^2/c^2$. The value for A_0 at 35° is 5.4×10^{-6}. For forward angles, as in our parity violation experiment, the asymmetry is most sensitive to F_1^s with small admixtures of F_2^s and G_A^s.

2 Experimental setup

2.1 Measurement principle

The experimental concept is very simple. It consists of counting the elastic scattered electrons N^+ and N^- for right- and left-handed polarized electrons and then getting the asymmetry in the cross-section by

$$A = \frac{N^+ - N^-}{N^+ + N^-}\,. \qquad (2)$$

For the desired statistical accuracy, about 2×10^{13} elastic electrons have to be counted. To achieve this within a measurement time of 1000 hours, a high luminosity of $L = 0.5 \times 10^{38}\ \mathrm{cm}^{-2}\mathrm{s}^{-1}$ is necessary. This luminosity leads to an elastic rate of about 10 MHz and a background rate of about 100 MHz in the detector.

Polarized electrons at a polarization between 75% and 80% are produced via photoeffect from strained layer GaAs-crystals. The electrons are then accelerated in the Mainz Microtron accelerator (MAMI) to an energy of 854.3 MeV. Helicity-correlated fluctuations of the beam are minimized by several stabilization systems. The small helicity-correlated fluctuations of the beam parameters are measured with high accuracy in our monitor system.

[a] e-mail: baunack@kph.uni-mainz.de

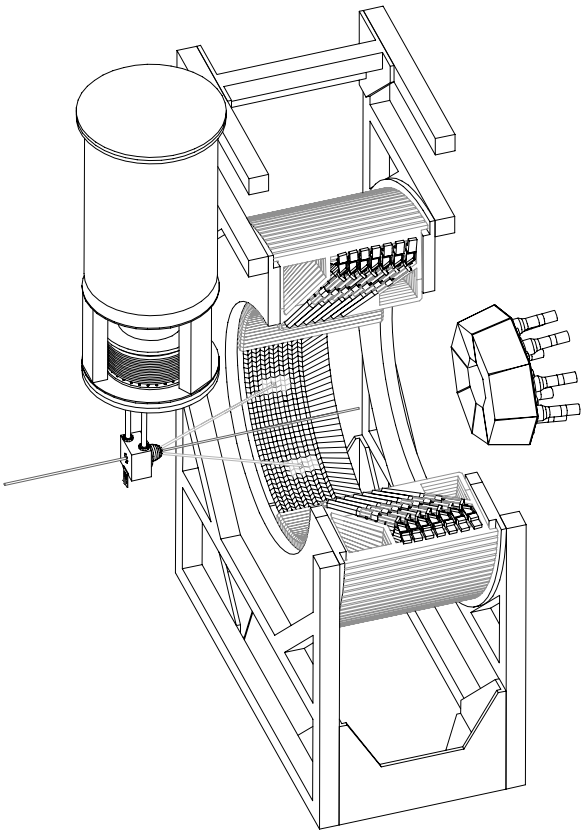

Fig. 1. Drawing of target, lead fluoride calorimeter and luminosity monitors.

In the measurements presented here the polarization of the electron beam has been measured with a Moeller polarimeter of the A1 Collaboration.

The electron beam hits the 10 cm long liquid-hydrogen target, which is designed to cool the 80 W of heating power from the 20 μA electron beam. The target does not show boiling, despite the fact that the beam is not rastered. The energy of the scattered particles is measured in our homogenous absorbing PbF_2 Čerenkov shower calorimeter. The luminosity is measured under small angles downstream of the target. The beam is dumped in a water-cooled beam dump.

2.2 PbF_2 calorimeter

The PbF_2 calorimeter is the central part of the MAMI parity experiment. It measures both position and energy of the scattered particles within a scattering angle between 30° to 40° within full azimuthal symmetry (total solid angle 0.7 sr). The energy and position signals are digitized and filled in histograms for positive and negative helicity states and stored on disk for later offline analysis. The calorimeter deals with high rates of about 100 MHz and provides an energy resolution of $3.5\%/\sqrt{E}$, which allows a separation of elastic scattered electrons from inelastic events. There are high demands on the calorimeter material as well as on the calorimeter electronics.

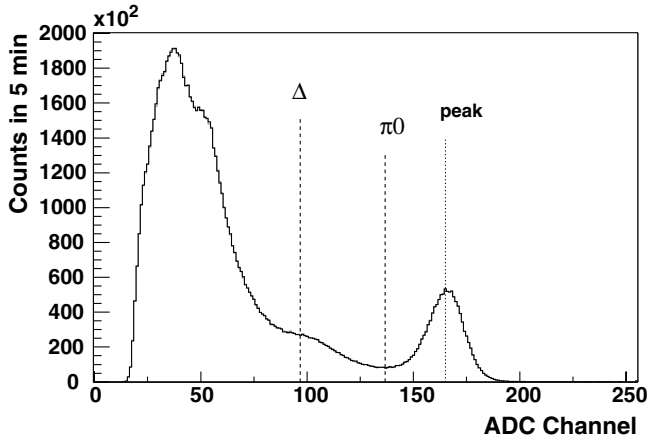

Fig. 2. Energy spectrum of the lead fluoride calorimeter. The spectrum is corrected for the differential non-linearities (DNL) of the ADC. x-axis = energy in ADC units. One can see the elastic peak at ADC channel 165, the π_0 production threshold at ADC channel 137 and the huge background. The cut-off at low ADC channels is due to thresholds in the electronics.

Lead fluoride (PbF_2) has been chosen as calorimeter material. PbF_2 has a high density and a short radiation length, as a pure Čerenkov radiator it is intrinsic fast and provides a good energy resolution. A schematic view of the PbF_2 calorimeter is shown in fig. 1. There are 1022 PbF_2 single crystals arranged in 146 columns and 7 rows.

For an almost complete coverage of the electromagnetic shower of an event, the signals of 3×3 crystals are summed up. This minimizes the energy loss, the energy resolution gets enhanced.

2.3 Electronics

The data acquisiton system has been developed at the Institute of Nuclear Physics, Mainz. Due to the high rates parallelisation of the electronics has been chosen. There are 1022 identical circuits, *i.e.* each crystal has such an electronics channel. The electronic circuit is divided into two parts, an analogue and a digital part. A dead time of 20 ns for the complete event is achieved. There is no individual channel information processed, each crystal is the center of a matrix of 9 channels and the analogue pulses of the matrix are summed by an analogue summing amplifier. The analogue summation signal is then digitized by a fast ADC. In addition, the center channel charge is integrated and also digitized. This gives information on the impact position on the individual crystal.

At the summation point of each channel, the analogue signals of the 8 direct neighbours need to be connected. Second hits within the integration time of 20 ns in the same crystal or in the a matrix of 25 crystals need to be recognised, so that on the veto level each crystals electronics circuit must be connected with the 24 neighbours. Due to this high connectivity, the topology of the electronics is the same as in the detector, a closed cylinder where neighbouring electronics channels correspond to neighbouring crystals in the detector.

Table 1. The table gives an overview over the small helicity-correlated fluctuations of the beam parameters and the resulting false asymmetries.

Parameter	Value	(False A)/A_0
I asym	$7.5 \cdot 10^{-8} \pm 2.3 \cdot 10^{-7}$	(0.9 ± 94.1) %
pos$X$ diff	(8.0 ± 1.0) nm	(0.3 ± 2.3) %
pos$Y$ diff	(82.2 ± 1.0) nm	(2.9 ± 6.0) %
angle$X$ diff	$(1.7 \cdot 10^{-7} \pm 1.8 \cdot 10^{-8})^\circ$	(0.1 ± 0.9) %
angle$Y$ diff	$(3.5 \cdot 10^{-7} \pm 2.2 \cdot 10^{-8})^\circ$	(0.3 ± 1.0) %
E diff	(5.2 ± 0.2) eV	(0.1 ± 0.3) %

2.4 Energy spectra

At the measurements presented here, one half of the PbF_2 calorimeter was equipped. Per run there are 1022 energy spectra as shown in fig. 2. With determination of the elastic line ("peak") the pion production threshold can be calculated. The knowledge of this threshold allows it to define an elastic cut and determine the counts of right- and left-handed elastic scattered electrons.

2.5 Beam parameters

Helicity-correlated beam fluctuations cause false asymmetries in the PbF_2 calorimeter. In order to control and minimize these beam fluctuations, beam monitor and stabilization systems for position, intensity and energy have been installed. Table 1 lists the achieved beam fluctuations and the resulting false asymmetries.

3 Analysis

In contrast to the simple approach in eq. (2), the elastic count rates are normalized to the target density $\rho = \frac{I}{I}$:

$$A_{\text{meas}} = \frac{\frac{N^+}{\rho^+} - \frac{N^-}{\rho^-}}{\frac{N^+}{\rho^+} + \frac{N^-}{\rho^-}} \,. \tag{3}$$

The asymmetry is extracted by a linear regression in multiple dimensions. There is a $\lambda/2$-wave plate, which can be inserted in the laser system of the electron source. With this $\lambda/2$-wave plate in, the helicity of the electrons is reverted. This change is not known to the electronics and an important test of the whole apparatus. The sign of the observed asymmetries should correspond to the position of this plate. We have 17 data sets, 9 sets with $\lambda/2$-wave plate out and 8 sets with $\lambda/2$-wave plate in. The resulting physical asymmetries should change their sign corresponding to the position of the $\lambda/2$-wave plate. Figure 3 shows the preliminary results of the ongoing analysis. The change of sign for the individual data sets can be observed very well. The preliminary physical asymmetry at 35° that we get from all data sets together is

$$A_{\text{phys}} = (-7.3 \pm 0.9) \times 10^{-6} \,. \tag{4}$$

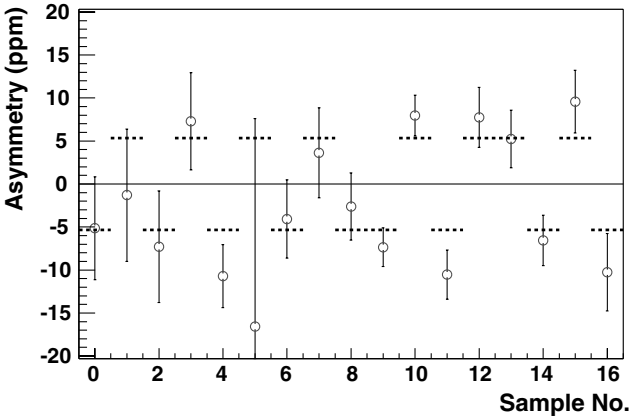

Fig. 3. Decorrelated physical asymmetries of the A4 experiment. The dashed lines indicate the expectation of the asymmetry without strangeness contribution.

The uncertainty in our result comes from three parts. One part arises from statistics, the correction for false asymmetries enters some error and the polarisation measurement contributes. The value of the asymmetrie has to be compared with A_0 without strangeness, 5.4×10^{-6}, which has some also some error due to the form factors that were put in to calculate A_0.

4 Outlook

The upgrade of the A4 experiment is currently on the way. The detector is fully equipped with all 1022 detectors and its electronics. The Compton backscattering polarimeter is being installed, which measures the absolute polarisation non-destructively during asymmetry data taking. Additionally, a Compton polarimeter is ready for installation downstream the calorimeter to provide fast measurements of relative changes in the beam polarisation. The future measurements will include

- measurements with increased statistics at 0.23 GeV under forward angles;
- 0.1 GeV under forward angles, which corresponds to the SAMPLE Q^2 under backward angles;
- 0.23 GeV under backward angles, which corresponds to our Q^2 under forward angles;
- 0.47 GeV under backward angles, which corresponds to the HAPPEX Q^2 under forward angles.

All these measurements together will allow for the first time a flavour separation of the form factors of the nucleon.

References

1. B. Borasoy, U.-G. Meissner, Ann. Phys. **254**, 192 (1997).
2. M.J. Musolf *et al.*, Phys. Rep. **239**, 1 (1994).